Chemical Science

ROYAL SOCIETY OF CHEMISTRY

MINIREVIEW

View Article Online
View Journal | View Issue

Cite this: *Chem. Sci.*, 2020, **11**, 12269

All publication charges for this article have been paid for by the Royal Society of Chemistry

Received 17th August 2020
Accepted 21st October 2020

DOI: 10.1039/d0sc04486e

rsc.li/chemical-science

Polydopamine-based nanoreactors: synthesis and applications in bioscience and energy materials

Shilin Mei,†[a] Xiaohui Xu,†[b] Rodney D. Priestley *[bc] and Yan Lu *[ad]

Polydopamine (PDA)-based nanoreactors have shown exceptional promise as multifunctional materials due to their nanoscale dimensions and sub-microliter volumes for reactions of different systems. Biocompatibility, abundance of active sites, and excellent photothermal conversion have facilitated their extensive use in bioscience and energy storage/conversion. This minireview summarizes recent advances in PDA-based nanoreactors, as applied to the abovementioned fields. We first highlight the design and synthesis of functional PDA-based nanoreactors with structural and compositional diversity. Special emphasis in bioscience has been given to drug/protein delivery, photothermal therapy, and antibacterial properties, while for energy-related applications, the focus is on electrochemical energy storage, catalysis, and solar energy harvesting. In addition, perspectives on pressing challenges and future research opportunities regarding PDA-based nanoreactors are discussed.

1. Introduction

As the major pigment of eumelanin which contains both catechol and amino groups, polydopamine (PDA) was first comprehensively researched by Messersmith *et al.* in 2007 as a multi-functional polymer coating atop various surfaces.[1] The early investigations of PDA primarily focused on surface modification and biological applications. In recent years, the unique properties of PDA and PDA-derived nanomaterials have been widely exploited to develop a range of catalysts and electrode materials for emerging energy-related applications. Currently, there exist several excellent reviews which summarize the synthetic routes, surface chemistry, and scope of application for PDA.[2–4] However, no review presents, in depth and breadth, the topic of PDA-based nanoreactors with nanoscale confining areas and the ability to encapsulate or load guest molecules, in aspects of their structure–property relationships and emerging applications. With the rise of nanoscience and nanotechnology, a variety of PDA-based nanoreactors have been developed using a range of geometries, such as nanopores, hollow nanoparticles, porous architectures, and tubular nanostructures. In addition, replicating structures native to

[a]*Department for Electrochemical Energy Storage, Helmholtz-Zentrum Berlin für Materialien und Energie, 14109 Berlin, Germany. E-mail: yan.lu@helmholtz-berlin.de*
[b]*Department of Chemical and Biological Engineering, Princeton University, New Jersey 08544, USA. E-mail: rpriestl@Princeton.EDU*
[c]*Princeton Institute of the Science and Technology of Materials, Princeton University, New Jersey 08544, USA*
[d]*Institute of Chemistry, University of Potsdam, 14476 Potsdam, Germany*
† These authors contributed equally.

Shilin Mei received his B.S. and M.S. degrees in Chemistry from Renmin University, China, in 2009 and 2012, respectively, and completed his PhD in 2017 with Prof. Matthias Ballauff at Humboldt University of Berlin, Germany. He worked on his postdoctoral research on energy storage materials in the Department for Electrochemical Energy Storage, Helmholtz-Zentrum Berlin für Materialien und Energie GmbH from 2017 to 2020. His research interests focus on functional hybrid nanomaterials and energy storage.

Xiaohui Xu completed her Ph.D. in 2019 in applied chemistry from Chang'an University, while undertaking thesis research at Helmholtz-Zentrum Berlin für Materialien und Energie in Germany. Then, she received Princeton's Presidential Postdoctoral Fellowship and joined Prof. Rodney D. Priestley's group as a postdoc in the Department of Chemical and Biological Engineering. At Princeton University, her postdoctoral research focus is on developing stimuli-responsive materials for environmental remediation.

biological systems offers a means of creating unique nanoscale chemical environments partitioned from the surrounding bulk space. PDA-based nanomaterials have important implications in many fields ranging from bioscience to energy fields. Specifically, there has been long-standing interest in constructing PDA-based multifunctional nanoreactors, which would require sophisticated design and complementary integration to achieve optimal synergistic performance.

In this context, utilizing the synergic effect of its intrinsic surface chemistry and structural versatility, PDA is of great significance for the rational design of multifunctional nanoreactors. PDA-based nanoreactors in different forms have been produced by a range of procedures, including direct polymerization, hard- and soft-templating, and self-assembly methods.[3] Although there exist PDA nanostructures that have been designed and explored for different applications, the essential role of structure or geometry on their properties has not been sufficiently highlighted.

The widespread application of PDA-based nanoreactors has rapidly advanced in recent years, as indicated by the large number of publications from 2007 to today. This trend reveals the global significance of PDA and the intense interest in scientific research in the field. In the ongoing research for PDA-based nanoreactors, bio-science and energy storage have emerged as important applications. The abundance of active sites, which could enable chemical reactions, as well as the ease of coating atop surfaces has spurred the extensive study of PDA in drug/gene delivery and controlled release, and antibacterial coatings.[2] Besides, due to its unique photothermal conversion properties, there are an ever-growing number of investigations on the use of PDA for photothermal therapy. Over time, PDA-based nanoreactors have found new applications in the field of electrochemical energy storage. As a high-yield carbon source with a high content of N-doping, PDA-derived carbon nanomaterials have been widely applied in rechargeable batteries and supercapacitors.[6–8] Recently, direct use of PDA in energy systems has gained increasing interest based on its unique chemical properties, such as efficient redox reactions of metal–ion batteries, and good affinity to intermediates of polysulfides of metal/sulfur batteries.[4] Other attractive fields involve catalysis and solar energy conversion/harvesting,[2–4] where a lot remains to be explored.

The current review surveys the progress of the above-mentioned specific fields in a comparative fashion and discusses the state-of-the-art understanding in each. We first highlight the delicate design and synthesis of functional PDA nanoreactors with structural versatility, which is facilitated by the intriguing physicochemical properties of PDA. Afterwards, the structure- and property-dominated applications of PDA nanoreactors with well-designed components and nanostructures are discussed in detail in the fields of bioscience and energy materials. We particularly focus on the function-oriented strategies for addressing the specific issues in their applications. At the end, we conclude with perspectives on pressing challenges and future research directions of PDA-based nanoreactors.

2. Synthesis strategies for PDA nanoreactors

Despite several proposed structures of PDA,[5–8] the molecular mechanism of polymerization has been a topic of scientific

Rodney D. Priestley is the Vice Dean for Innovation at Princeton University. He is also a Professor in the Department of Chemical and Biological Engineering and the Associate Director of the Princeton Center for Complex Materials. He obtained his Ph.D. in Chemical Engineering from Northwestern University in 2008. His research involves the description and development of complex materials, especially nanoparticles, thin polymer films, and nanocomposites, with particular focus on behavior in confinement and at interfaces. His work is making an impact on industries ranging from personal care to aerospace. His recent interests include the use of polymers for sustainability and their impact on the environment. Recent recognitions include the 2020 American Physical Society Dillon Medal and 2020 ACS Macro Letters/Biomacromolecules/Macromolecules Young Investigator Award. Priestley was also named to the Root 100 list of most influential African Americans and recognized as a World Economic Forum Young Scientist.

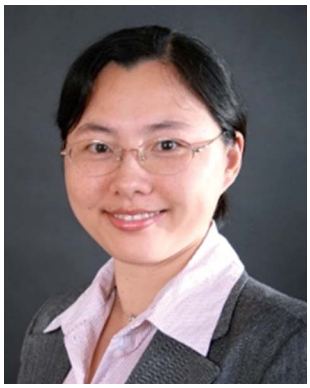

Yan Lu received her PhD in 2005 with summa cum laude under the supervision of Prof. H.-J. P. Adler at Dresden University of Technology, Germany. After that, she worked first as a post-doc and then a research scientist in Prof. Matthias Ballauff's group at the University of Bayreuth. In 2009, she joined Helmholtz-Zentrum Berlin für Materialien und Energie (HZB) as a group leader in Colloid Chemistry. She was selected as a top female researcher (W2/W3-Programme) in the Helmholtz Association in 2015. Since 2017, she has been a professor in the Institute of Chemistry at the University of Potsdam. Since 2019, she has been the Head of Department for Electrochemical Energy Storage at HZB. Her research interests include design and synthesis of functional hybrid materials based on polymeric colloidal particles with versatile applications, such as energy storage materials, catalysts, sensors and optical devices.

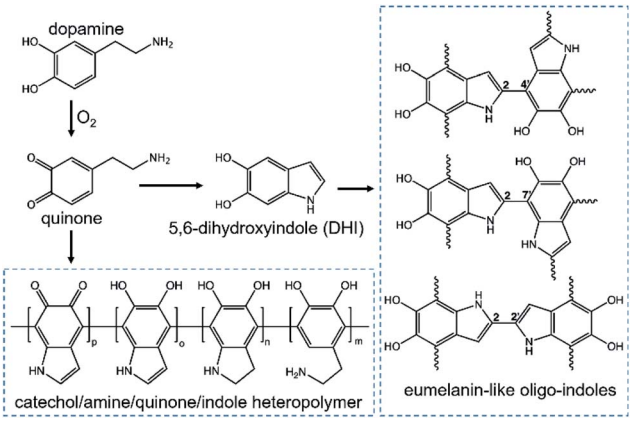

Scheme 1 Proposed formation and chemical structures of PDA. Intermediates from auto-oxidation: quinone and 5,6-dihydroxyindole; possible structures from covalent coupling of intermediates: catechol/amine/quinone/indole heteropolymer or eumelanin-like oligo-indoles. Reproduced with permission.[9] Copyright 2018, American Chemical Society.

debate due to the complex redox process as well as the generation of a series of intermediates. Scheme 1 illustrates the current research on the formation and chemical structure of PDA.[9] In view of several excellent reviews presenting the surface chemistry in a comprehensive manner,[2,9,10] we focus on the synthesis protocols that result in the formation of PDA nanoreactors in the absence or presence of templating agents (*e.g.* block copolymers, polyelectrolytes, surfactants, proteins, and even some small organic molecules). We will also describe the use of thin PDA layers to coat already synthesized nanoparticles or nanotubes to generate PDA-based nanoreactors.

Most PDA nanostructures can be produced from oxidative polymerization of dopamine in the presence of Tris buffer at pH $\sim$ 8.5 by using O_2 dissolved in water as the oxidant. The synthesis was further improved with the use of water–ethanol mixtures by adding ammonia as a catalyst in the dopamine-containing solution.[2,3] Besides O_2 dissolved in water, several other oxidants can be used as well, such as ammonium peroxodisulfate and sodium periodate,[11] or UV irradiation to generate free radical species.[12] The type of oxidant has a major impact on the kinetics of PDA formation. Therefore, consideration should be given to controlling the precise reaction conditions when forming PDA into nanostructures for various applications. Note that other methods including hydrothermal synthesis (under acidic conditions),[13] electropolymerization,[14] and biosynthesis based on enzymes[15] are also effective strategies to generate PDA. However, one limitation of these methods is their specified experimental conditions, which may hinder their application as a generalized approach for the synthesis of well-defined PDA nanoreactors, and thus they are not emphasized here.

Without templating agents, PDA itself can form different structures, including size-tunable spheres, nanofibers, nanofilms, *etc.*[16–20] The presence of small molecules such as folic acid and DNA origamis was found to impact the size and morphology of PDA assemblies.[18,21] For instance, PDA nanofibers could be obtained by introducing folic acid into dopamine in Tris buffer. In this method, the folic acid facilitated the formation of nanobelts and nanosheets through π-stacking with small self-assembled aggregates of oxidized dopamine.[18] Surfactants, such as sodium dodecyl sulfate (SDS) and hexadecyltrimethylammonium bromide (CTAB), have enabled accelerated dopamine oxidation, thus resulting in smaller PDA aggregates.[22]

With the assistance of templates, PDA can be manufactured into various desired structures from nano- to macro-size due to its unique adhesive properties and film-forming ability. These properties have been utilized to develop a broad range of architectures for desired applications, such as nano/microcapsules, nanotubes, hollow structures, and porous structures.[23–27] Despite the advantage of precise control over morphology, there is a major drawback in applying inorganic hard templates, which mainly arises from the need to remove the sacrificial hard templates by harsh chemical treatment. Therefore, these hard templates are usually involved in the final product either as catalytically active or magnetic cores (Fig. 1a),[28] or as a structure-stabilizing agent (Fig. 1b).[29] In contrast, the soft template strategy has been considered as the main technique to synthesize complex nanostructures of PDA. This inspired the investigation of PDA in dopamine solutions containing emulsion droplets, synthetic polymers, polyelectrolytes, or proteins.[30–33] For instance, the formation of PDA mesostructures using single micelle-directed assembly has been intensively studied due to their highly tunable porous structures. The process involves three steps: (1) the formation of micelles from surfactants or block polymers, (2) the interaction between micelles and oligomers to form micelle–oligomer composites, and (3) the sequential crosslinking between the micelle–oligomer composites to form mesoporous materials. These steps are independent, and differ from the conventional co-assembly mechanisms. For example, using the emulsion-directed assembly of Pluronic F127, mesitylene and PDA, mesoporous PDA NPs with diameters of $\sim$200 nm and radial mesopores of $\sim$11 nm were obtained.[22,27] By combining two similar block copolymers (Pluronic P123 and Pluronic F127) with PDA oligomers and mesitylene, walnut-like mesoporous PDA particles with diameters of $\sim$270 nm and bicontinuous channels ranging from $\sim$20 to 95 nm were formed (Fig. 1c).

Although soft templates such as surfactant droplets and polymer micelles can be removed by extraction, evaporation, or dissolving with a selective solvent, these soft templates usually give rise to simple nanostructures such as hollow or porous particles. Therefore, it is of great importance to understand the trade-off between applying a soft template and creating complex nanostructures of PDA. Recently, a PDA-based catalytic nanoreactor with an interconnected tunnel structure was reported using porous polystyrene-*block*-poly(2-vinylpyridine) particles derived from a selective swelling process to serve as a soft template (Fig. 1d).[34] The advantage of using block copolymer assemblies, which have highly tunable nanostructures and are easily removed by organic solvents, is that more complex structures can be obtained. This strategy enables us to circumvent the aforementioned synthetic challenges by using block copolymer assemblies as soft templates, which can

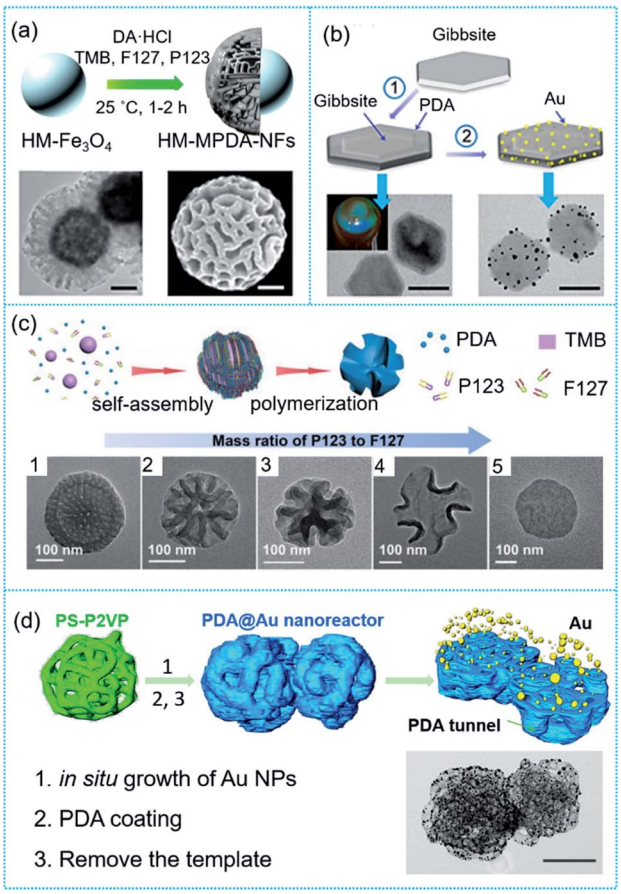

Fig. 1 Different synthetic routes of PDA-based nanoreactors. (a) One-step synthesis of magnetic flower-like PDA particles. The scale bar is 100 nm. Reproduced with permission.[28] Copyright 2019, American Chemical Society. (b) Templated synthesis and structure of the gibbsite-PDA–Au core–shell nanoplates. The scale bar is 100 nm. Reproduced with permission.[29] Copyright 2015, American Chemical Society. (c) Cooperative assembly of P123 and F127, PDA oligomers and trimethylbenzene into walnut-shaped macro-/mesoporous PDA particles. Reproduced with permission.[27] Copyright 2018, Wiley-VCH. (d) Polystyrene-*block*-poly(2-vinylpyridine) porous particles as a template for the synthesis of PDA@Au nanoreactors with an interconnected tunnel structure. The scale bar is 200 nm. Reproduced with permission.[34] CCBY.

produce PDA nanoreactors with complex nanostructures and preserve the functionality of the PDA for further use.

The wide range of structure- or morphology-oriented applications of PDA-based nanoreactors also derive from their unique chemical properties. Robust nanostructures are required in most applications including bioscience and energy materials. Fortunately, PDA is stable between pH 2 and 11 and within a wide temperature range.[2–10] In addition, unlike many polymers, PDA is insoluble in most of the commonly used organic solvents, including tetrahydrofuran (THF), acetone, *N*,*N*-dimethylformamide (DMF) and so on. However, PDA is degradable under strong alkaline conditions (*e.g.* 1 M NaOH solution) or in the presence of oxidizing agents such as H_2O_2 and free radicals in the human body. Such degradation can actually be a merit rather than a drawback when applied in biomedical applications. Other unique properties such as biocompatibility, adhesive capability, reducing ability, and photothermal conversion properties of PDA have triggered the fast development of its applications in bioscience and energy fields.

3. Applications in bioscience

As a natural melanin-like biopolymer produced by auto-oxidation of dopamine, PDA possesses excellent biocompatibility and low cytotoxicity, making it a promising candidate for biomaterials. Thus, there has been a rapid growth in the design of PDA nanostructures in biomedical fields such as drug/protein delivery, photothermal therapy, and antibacterial materials. In the following sections, the recent developments of PDA-based nanoreactors for bioscience applications in the past several years are discussed.

3.1 Drug/protein delivery applications

In cancer therapy, constructing a nanocarrier delivering antitumor drugs is an appealing and potential way to realize improved bioavailability, reduced toxicity, sustained activity, simplified dosing regimens, improved patient adherence, and enhanced overall efficacy.[35] As a novel nanocarrier, PDA is rich in aromatic rings, and amino and hydroxyl groups, providing plentiful active sites for binding various drugs and chemical molecules *via* π–π stacking and/or hydrogen bonding.[36–38] To date, a wide range of antitumor drugs such as doxorubicin (DOX),[39] 7-ethyl-10-hydroxycamptothecin (SN38),[40] bortezomib,[41] terbinafine (TBF),[42] docetaxel (DTX), and dihydroartemisinin (DHA),[43] and recombinant proteins such as green fluorescent protein (GFP), ribonuclease A protein (RNase),[44] and antigen-ovalbumin (OVA)[38] have been delivered to targeted tumor sites by PDA nanostructures. Moreover, PDA can be easily synthesized into various nanostructures, which strongly influences their drug loading performance and release function owing to their controllable surface area and tunable surface properties. Based on such properties, we classify them into four categories for the following discussion, namely PDA nanospheres, core–shell nanocomposites, hollow PDA nanocapsules and mesoporous PDA nanostructures.

Particularly, PDA colloidal nanospheres 70 to 400 nm in size can be obtained simply by oxidative self-polymerization of dopamine in a mixed solvent of water and ethanol at room temperature. As a catecholamine polymer, the resultant PDA NPs could be covalently bound to the free amino and thiol groups of the tumor model antigen-ovalbumin (OVA).[38] Thus, PDA NPs with a strong antigen loading capacity have great potential as a subcutaneous antigen delivery vehicle in antitumor therapy. Another type of interaction between PDA and chemical drugs relies on π–π stacking and/or hydrogen bonding, which endows PDA with superior drug loading capability and pH-responsive release properties. By simply incubating PDA with anticancer drugs in aqueous solution, PDA-polyethylene glycol (PEG) microspheres could easily load DOX and 7-ethyl-10-hydroxycamptothecin, and trigger their release

under acidic conditions (pH = 5.0).[40] The acid triggered drug release behavior is observed because at low pH, the π–π interactions between PDA and drugs are partially destroyed due to the protonation of amino groups on the PDA scaffolds and/or on the DOX molecules. This stimulus release strategy could facilitate the release of anticancer drugs at the tumor site and significantly enhance drug utilization and improve the therapeutic efficacy.

PDA coatings are another intensively used class of nanoreactors in drug delivery applications. Owing to the simple yet versatile method of fabrication and its surface adherence properties, PDA has been most widely used for the functionalization and/or coating of various other nanostructures to manipulate their drug delivery behavior.[45–47] As popular magnetic substrates, Fe_3O_4 NPs were coated with a PDA shell layer and then applied as a carrier for the anticancer drug bortezomib to control the drug release behavior[41] (Fig. 2a and b). PDA can also deposit tightly on poly(lactic-*co*-glycolic acid) NP surfaces *via* covalent and noncovalent interactions, forming a durable layer that serves as an intermediate for ligand incorporation.[46] The PDA shell layer can bind amine-terminated functional ligands such as a small molecule (*e.g.*, folate), a peptide, and a polymer [poly(carboxybetaine methacrylate)] *via* Michael addition and/or Schiff base reactions, resulting in a long half-life and high cellular uptake.

The other two widely reported types of PDA nanoreactors are hollow PDA nanocapsules and mesoporous PDA with higher surface area and more inner void space that are beneficial for drug molecule loading. The frequently employed method to prepare PDA nanocapsules is to deposit a PDA shell layer atop the surface of soft or solid spherical templates, followed by removal of the inner template.[23,48] As an example, monodisperse hollow PDA nanocapsules with sizes of 400 nm to 2.4 μm were obtained using an emulsion of dimethyldiethoxysilane droplets as soft templates.[49] The PDA capsules can immobilize the thiolated poly(methacrylic acid)–doxorubicin conjugate *via* robust thiol–catechol reactions (Fig. 2c and d). Notably, the hollow PDA nanoreactors displayed excellent loading efficiency and the loading capacity was calculated to be 557.8 mg g^{-1}, which is 5.7 times more than that of PDA nanoparticles. Recently, core–shell Au@PDA mesoporous nanoparticles with plasmonic cores and mesoporous polydopamine shell layers were developed for tailored loading and release of recombinant proteins, green fluorescent protein (GFP), and ribonuclease A protein, *in vitro* and inside a solid tumor (Fig. 2e and f).[44] Taken together, these results imply that PDA-based functional nanoreactors are a promising candidate for further cancer therapy.

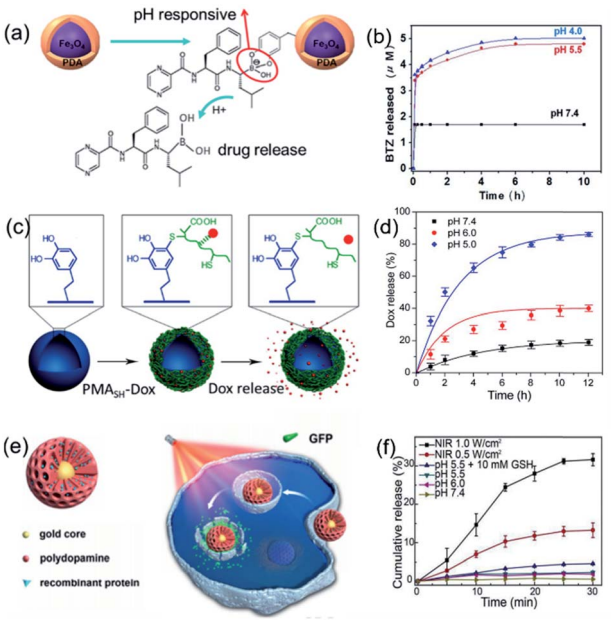

Fig. 2 Schematic illustrations for the synthesis, morphology and drug release behavior of (a and b) PDA coated Fe_3O_4 nanoreactors. Reproduced with permission.[41] Copyright 2014, American Chemical Society. (c and d) Hollow PDA nanoreactors. Reproduced with permission.[49] Copyright 2012, Royal Society of Chemistry. (e and f) Mesoporous Au@mPDA NPs. Reproduced with permission.[44] Copyright 2016, American Chemical Society.

3.2 Photothermal therapy

Photothermal therapy (PTT), which employs photoabsorbers to convert light energy into thermal energy to "heat" tumor cells, is emerging as a powerful technique for cancer treatment because of its high selectivity and minimal invasiveness. Compared with traditional techniques, the therapeutic effects of photothermal therapy occur only at the tumor sites, effectively avoiding the risks of killing normal cells and destroying the immune system. In the mechanism of PTT, photothermal agents and a near-infrared (NIR) laser are primary components. Photothermal agents can absorb near-infrared light and generate efficient hyperthermia to augment tumor vascular permeability, and thereby promote the delivery of medication toward tumor sites to improve therapeutic efficiency and reduce side-effects.[50–52]

PDA exhibits broad absorption ranging from ultraviolet (UV) to NIR wavelengths and shows a photothermal conversion efficiency of 40%, much higher than that of conventionally and widely used gold nanorods (22%).[53] When applied in *in vivo* cancer photothermal therapy, PDA NPs could efficiently kill cancer cells and suppress tumor growth without damaging healthy tissues. Notably, a high power density (808 nm, >2 W cm^{-2}) was usually necessary for unmodified PDA NPs for efficient cancer PTT treatment. This strong irradiation can damage normal tissue and induce serious side effects.[54–56] An efficient way to improve PTT treatment with low laser energy density for cancer theranostics is integrating indocyanine green with PDA-Fe^{3+} NPs.[54] In contrast to pure PDA NPs, the NIR optical absorption of indocyanine green-loaded PDA-Fe^{3+} NPs increased nearly 6 times and the temperature readily reached 55.4 °C upon laser irradiation with low energy density (808 nm, 1.0 W cm^{-2}, 10 min). The enhanced photothermal effect upon integration of indocyanine green with PDA was also demonstrated by other researchers.[55,56] PDA-coated magnetic composite particles also exhibited an increased NIR absorption and intense local hyperthermia (>50 °C) to destroy the tumor tissues efficiently.[57]

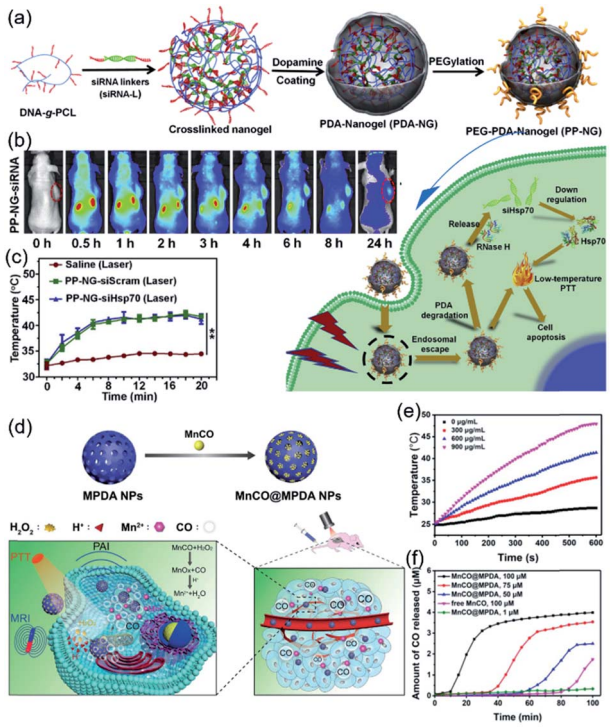

Fig. 3 (a) Synthetic route to PDA-coated nucleic acid nanogel with a PEGylated surface (PEG-PDA-Nanogel) and the mechanism of siRNA-mediated low-temperature photothermal therapy. (b) *In vivo* fluorescence images of HeLa tumor-bearing mice after intravenously injecting PP-NG-siRNAs. (c) Changes of the tumor temperature with time. Reproduced with permission.[58] Copyright 2020, Elsevier. (d) Schematic illustrations of MnCO@MPDA particles for CO/PTT combination therapy of tumors. Temperature elevation (e) and CO release (f) of MnCO@MPDA particles. Reproduced with permission.[64] Copyright 2019, Wiley-VCH.

The high local temperature at the tumor site will increase the temperature of the surrounding normal tissue *via* thermal diffusion, which potentially induces local inflammation and tumor metastasis. To avoid these side effects, a PDA-coated nucleic acid nanogel was designed as a therapeutic complex for siRNA-mediated low-temperature PTT (Fig. 3a and b).[58] To verify siRNA-mediated low-temperature PTT *in vitro*, HeLa cells were incubated with nanogel-PDA and then irradiated with 808 nm laser (0.5 W cm^{-2}, 20 min). The results show that the anti-Hsp70 siRNA bearing nanogel-PDA can induce efficient target gene knockdown and apoptosis based photothermal cell killing rather than cell necrosis under mild conditions.

During the past few years, PTT combined with other therapeutic means such as chemotherapy, immunotherapy and carbon monoxide (CO) therapy to treat tumors has attracted increasing attention. Combination therapy can efficiently enhance anticancer efficacy and reduce side effects.[56–63] To realize the combination of PTT and chemotherapy, photothermal PDA NPs functionalized with glucose were loaded with the anticancer drug bortezomib through the acid-sensitive borate ester bond.[59] The combined chemo-photothermal therapy could promote photothermal heating and burst drug release, and further induce the tumor growth inhibition by ~104.7% with minimal side effects.

Apart from conventional anticancer drugs, CO-generating molecules were recently found to have antitumor effects by releasing the CO toxin into tumor cells. The generated CO can kill cancer cells by detracting the oxygen binding of hemoglobin and inhibiting cellular protein synthesis and decrease cell viability, proliferation and survival. To achieve a synergistic anticancer effect of PTT and CO therapy, the H^+/H_2O_2-responsive manganese carbonyl (MnCO) was encapsulated in the pores of mesoporous PDA (MPDA) NPs through hydrophobic interactions (Fig. 3c–e).[64] When the as-prepared MnCO@MPDA NPs were delivered to the tumor, MnCO reacted with H_2O_2 at tumor sites to produce toxic CO *via* a Fenton-like reaction, and induced reactive oxygen species-driven cancer cell apoptosis without affecting normal cells. Simultaneously, MnCO@MPDA NPs can effectively convert the locally applied NIR light to heat for tumor thermal treatment.

3.3 Antibacterial effect

Infections caused by various pathogenic bacteria and multidrug-resistant bacterial strains have resulted in numerous cases of morbidity and mortality clinically, posing a serious threat to public health. Therefore, there is an urgent need to design new and effective antibacterial materials for preventing the increasing prevalence of bacterial infections. To date, there has been growing interest in incorporation of antibacterial metals such as Cu, Ag, Au, and Zn, and antimicrobial enzymes such as lipase and lysostaphin as well as amino acids into PDA substances to enhance their stability and antibacterial activity.[65–73] In addition to the aforementioned conventional antibacterial agents, nitric oxide (NO), an endogenously produced molecule, exhibits more efficient antibacterial effects against both Gram-positive and Gram-negative bacterial species by inducing oxidative stress or nitrosative stress. Hollow PDA nanoparticles,[74] PDA-coated iron oxide nanoparticles,[75] and poly(ethylene glycol) grafted PDA coating layers[76] were functionalized with NO precursors/donors (*N*-diazeniumdiolate) to enhance antibacterial properties. Hence, using PDA as a NO carrier has opened up new opportunities in effective NO delivery and biofilm treatment.

It is important to stress that PDA is not only used as a carrier but can also serve as a heating center for photothermal treatment of microbes with the assistance of NIR light.[77–79] The NIR-induced burst NO release and hyperthermia could achieve synergistic bacterial inactivation, which is different from current NO-releasing platforms. Instead of directly immobilizing NO precursors atop PDA, a third-generation dendritic poly(amidoamine) (PAMAM) was introduced atop the surface Fe_3O_4@PDA particles and subsequently loaded with NO *via* the secondary amino groups of PAMAM (Fig. 4a).[80] The dendrimer modification significantly enhanced the NO payload capacity by 3 times, and the obtained platform exhibited a photocontrollable NO release (Fig. 4b and c). As visualized in Fig. 4d and e, the blue color of biofilm became significantly pale and very little biofilm biomass was detected after treatment. Taken together,

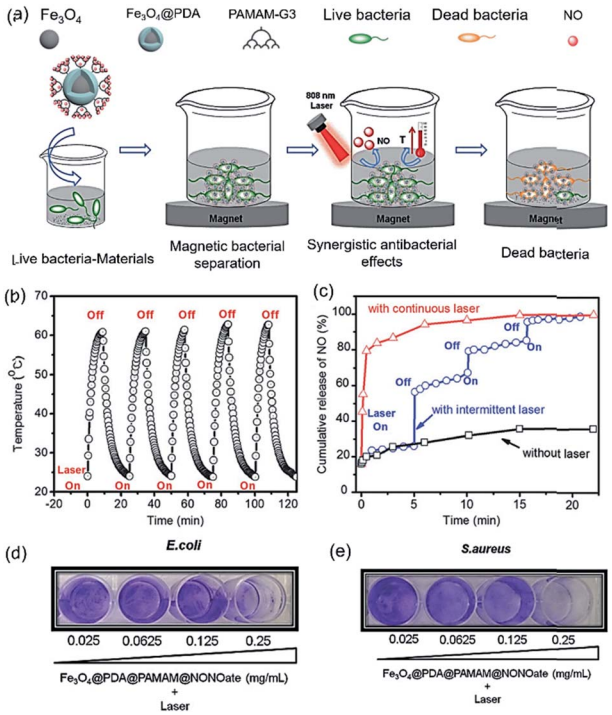

Fig. 4 (a) The synergistic photothermal/NO killing of bacteria of Fe_3O_4@PDA@PAMAM@NONOate and (b) photothermal stability evaluation of Fe_3O_4@PDA@PAMAM with five times laser switch-on and switch-off treatment. (c) NO release profile of Fe_3O_4@PDA@PAMAM@NONOate under different laser irradiation conditions. (d and e) Concentration-dependent bacterial biofilm eradication effect of Fe_3O_4@PDA@PAMAM@NONOate with 808 nm laser irradiation against *E. coli* (d) and *S. aureus* (e). Reproduced with permission.[80] Copyright 2018, Wiley-VCH.

these results indicate that the integration of NO and PDA could effectively eliminate bacteria more than the corresponding individual therapies.

In short, the various forms of PDA nanoreactors such as PDA NPs, hollow capsules and other PDA-coated nanocomposites have become highly versatile and powerful platforms for targeted drug delivery, photothermal cancer treatment, and antimicrobial applications. In addition to its rich surface properties, the discovery of its photothermal effect greatly boosts the further application of PDA in bioscience fields. Although exciting results have been achieved so far for the PDA-based nanoreactors, several problems remain unresolved and need to be investigated further. For instance, it is hard to evaluate/directly compare photothermal therapy among all the reported results, because the photothermal effect of PDA NPs or PDA-coated nanostructures differs in terms of particle diameter, coating thickness, cavity or porosity and material concentration. Furthermore, photothermal therapy experiments are often performed under different irradiation times and laser power densities, which makes it hard to compare their photothermal killing efficiency. In addition, detailed information regarding the pharmacokinetics behavior and long-term toxicity data of PDA-based materials are still lacking, which is a crucial aspect to ensure the success of PDA for biomedical applications.

4. Applications in energy

PDA has shown many potentially exciting applications in the exploration of new energy resources. Most work in this direction has concentrated on the utilization of the unique properties of PDA including the high carbonization yield, and robust wetting and adhesion capabilities, as well as its functions as a reducing agent and hydrogen bonding site. Although PDA-derived carbon materials have a large range of applications in electrochemical energy storage, such applications have been summarized in existing reviews,[2,4] and therefore will not be fully discussed here. This section specifically presents the applications of PDA in the generation of new energy sources based on its chemical properties in three fields including electrochemical energy storage, catalysis, and solar energy harvesting.

4.1 Electrochemical energy storage

4.1.1 Li-ion batteries. High capacity lithium ion batteries are in high demand because of recent advances in electric vehicles and mobile electronics. Significant improvements in their performance including energy and power density, cycle life, and safety reliability are highly desirable, particularly for future emerging markets.[81] Beyond its intensive use as a N-doped carbon source for advanced anodes,[4] PDA has also been employed in separators,[82,83] current collectors,[84] and lithium protecting layers[85] due to its versatility and wet-resistant adhesion ability. Recently, PDA-based nanoreactors encapsulated with active particles as anode materials have been employed to pursue excellent capacity and retention by effective stress relaxation and surface passivation.[86–88] In a recent study, graphene-wrapped PDA was directly coated atop silicon NPs as a buffer layer for lithium ion batteries (Fig. 5a).[87] The expansion cavities for silicon NPs during the charging and discharging process were provided by the graphene-wrapped PDA buffer layers. As a soft and elastic polymer, PDA can intrinsically allow for a relatively large volume change arising from the contraction and expansion of active materials through adjusting its own elastic deformation, thereby releasing the partial pressure of active materials during the charge/discharge process.[86] A second advantage involves prevention of direct contact between the active material and the electrolyte, thus eliminating the occurrence of side reactions at the electrode–electrolyte interface. The third benefit is that the construction of two stable interfaces between the active material and the buffer layer, as well as interactions between the buffer layer and the binder through coordination and a cross-link reaction, is helpful to improve the stability of the entire electrode system and thus prolong the electrode's cycle life.

In addition to electrode materials, there has been long-standing interest in PDA modified multifunctional separators due to their success in increasing the uptake amount of electrolyte, mechanically stabilizing the whole framework of the separators, and efficiently restraining the Li dendrite growth on

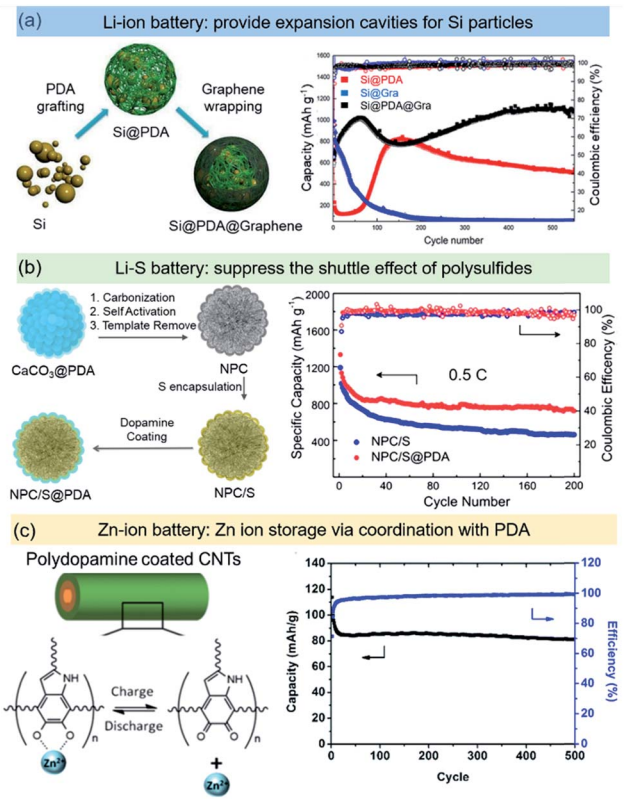

Fig. 5 PDA based nanoreactors for different types of batteries. (a) Si@PDA@graphene particles as an electrode material for Li-ion batteries. Reprinted with permission.[87] Copyright 2019, Wiley-VCH. (b) PDA as a coating layer to suppress the polysulfide shuttling in Li–S batteries. Reprinted with permission.[91] Copyright 2019, Wiley-VCH. (c) A PDA@CNT binder-free electrode for Zn-ion batteries. Reprinted with permission.[99] Copyright 2019, Royal Society of Chemistry.

the surface of Li metal.[83] In these studies, PDA is mainly used for the surface modification of separators or interlayers. PDA-based nanoreactors have not been fully employed in research of this type.

4.1.2 Li–S batteries. Li–S batteries have been considered as alternatives to lithium ion batteries due to their high theoretical capacity, but unfortunately suffer from the high electrical resistance of insulating sulfur, a large volumetric expansion (~80%), and a shuttle effect triggered by the dissolution of lithium polysulfide intermediates.[89] Encapsulating sulfur into PDA-derived carbon nanoreactors has become a popular strategy to address the above issues through suppressing the polysulfide diffusion and building a conductive framework for electron/ion transport.[90–93] Compared to PDA-derived carbon materials which provide mainly physical confinement for polysulfides, direct use of PDA has been found to be more efficient in adsorption of polysulfides *via* chemical confinement. The nitrogen and oxygen atoms with lone electron pairs in PDA can provide polar surfaces to trap polysulfide species; the strong chemical interactions between the nitrogen/oxygen atoms and lithium polysulfides can efficiently decrease their dissolution, thereby increasing sulfur utilization and improving the cycling stability. Similar to the function in Li-ion batteries, PDA-based sulfur cathodes also benefit from strong adhesion capability and flexibility, improved compatibility with electrolytes, and good lithium ion conductivity. Apart from the advantages discussed above, sulfur-containing nanoreactors with core/shell or porous structures exploit the mechanical flexibility of PDA for accommodating the volume changes of sulfur species during discharging and charging. A typical work demonstrating its multifunctional role was reported by Zhang *et al.*[91] PDA-coated N-doped hierarchical porous carbon spheres (NPC@PDA) with a core–shell structure were applied as a cathode material (Fig. 5b). The porous structure of PDA and N-doping of the carbon sphere core dramatically enhanced the chemical adsorption ability towards lithium polysulfides and the electrochemical reaction kinetics of sulfur, respectively. Similar studies have also been performed by Tu *et al.*[92] and Chen *et al.*[93] using S/C@PDA and S@PDA nanoreactors as cathode materials, respectively. These results demonstrate that sulfur-encapsulated PDA nanoreactors have great potential as a low-cost cathode in high-energy Li–S batteries.

Consistent with the improved electrochemical performances, the favorable interactions between Li_2S_x ($1 \leq x \leq 8$) species and PDA have been revealed by theoretical calculations.[93] Density functional theory (DFT) calculations indicated that the lone electron pairs on the electronegative N and O atoms in PDA were capable of binding with the Li of Li_2S_x ($1 \leq x \leq 8$), forming coordination-like interactions (N–Li, O–Li and N–Li–O). One lithium ion on one end point of a polysulfide bonds with N and O atoms in the PDA. Chen *et al.* summarized the calculated binding energies (E_b) of the polysulfides (Li_2S_8, Li_2S_6 and Li_2S_4) and of Li_2S bonded to PDA.[93] All of the E_b values were positive, indicating that PDA could act as an effective Li_2S_x reservoir for a highly reversible Li–S cathode. In addition, the calculation results for the interaction of Li_2S_8 and PDA demonstrated that the Li ions of Li_2S_8 could also bind with oxygen.

Despite solid study on the interactions of lithium polysulfides with PDA, the poor conductivity has always been the main drawback of PDA for electrochemical energy storage, hindering fast kinetics for the redox reactions of sulfur species. A trade-off between high capacity and long cycle life may remain a long-standing challenge when using PDA nanoreactors with sulfur host materials.

4.1.3 Other batteries. Apart from being employed in Li-ion and Li–S batteries, PDA has also been explored as an efficient electrode material for zinc–air batteries and sodium ion batteries.[94,95] For example, Wan *et al.* reported a N-doped carbon shell encapsulating metallic Co_2Fe_1 NPs in a small uniform size of 15 ± 5 nm and high density (metal loading up to 54.0 wt%) for zinc–air batteries using PDA as a protecting shell and heteroatom-doped carbon source.[94] A record power density of 423.7 mW cm^{-2} was achieved, for which they speculated that the complete graphitic carbon shells effectively prevented the corrosion and oxidation of metallic cores. Another inspiring study proposed that the controllable partial oxidation of PDA played a key role in balancing the proportion of redox-active carbonyl groups and the structural stability and conductivity of the electrode when used for sodium ion batteries.[95]

Unexpectedly, the optimized PDA derivative endows sodium-ion batteries with superior electrochemical performances, including high capacities (500 mA h g^{-1}) and good stable cyclability (100% capacity retention).

Zinc based aqueous batteries are being extensively investigated due to potential advantages in cost, safety, abundancy, and environmental friendliness.[96,97] With a very negative electric potential of ~0.76 V *vs.* standard hydrogen electrode (SHE), zinc based batteries also offer highly competitive energy densities. Very recently, an attempt has been made to develop PDA-based electrodes for Zn-based aqueous batteries. It has been demonstrated that quinone exhibits ion storage capability by coordination with its oxygen atoms when the carbonyl groups are reduced at low potentials. Both high capacity and cycling stability have been achieved with calix[4]quinone (C4Q) when used in a zinc ion battery.[98] Moreover, PDA is expected to have minimal dissolution in the electrolyte and long cycle life due to the stable, covalently connected structure. For instance, Liu *et al.* demonstrated a flexible, free-standing, binder-free PDA cathode fabricated with CNTs as a support for high-performance aqueous Zn-ion batteries (Fig. 5c).[99] The PDA delivers a low-rate specific capacity of 126.2 mA h g^{-1}. After an initial stabilization period, outstanding long-term stability was observed: after 500 cycles, the PDA electrode still retained 96% of the stabilized capacity. CV studies indicated that the electrode reaction was a surface process, similar to that in electrochemical capacitors. FT-IR and XPS studies have established the reaction mechanism to be a redox reaction between catechol and *ortho*-quinone accompanied by zinc ion adsorption and desorption. Therefore, the non-toxic, flexible PDA has great potential to broaden the application spectrum of aqueous zinc ion batteries.

4.2 Catalysis

4.2.1 Supporting materials for metal NPs. Metal NPs are widely used as efficient catalysts for small molecule reactions. To avoid the aggregation of metal NPs in solution, catalysts are usually stabilized by various types of supporting materials, ranging from inorganic to organic frameworks and coating layers. As discussed in Section 2, PDA shows great potential as a novel supporting material for metal nanocrystals due to its ability to reduce numerous types of metal ions.[100,101] Generally, PDA prevents the catalysts from aggregating and gathers reagents efficiently due to its high physical adsorption ability. In addition, the effect of PDA surface chemistry on inorganic nanocrystals has been investigated for advanced catalytic systems based on its tunable charge and conjugated structure.

A typical application of such PDA supported metallic catalyst is the catalytic degradation of organic pollutants such as nitroarenes and dye contaminants. The reduction of 4-nitrophenol by $NaBH_4$ was chosen as a model reaction for proving the concept. Noble metals of Au, Pt, Pd, Ag and their bimetallic nanoparticles stabilized by PDA have been used to reduce 4-nitrophenol in the presence of $NaBH_4$.[102] Besides removal of pollutants from water, PDA supported metal catalysts have been demonstrated to promote many kinds of heterogeneous catalytic transformations, including Suzuki couplings, catalytic transfer hydrogenation (CTH) reactions, Heck reactions, and other reactions with high efficiency.[103,104]

The synergistic effect of PDA and inorganic crystals on catalytic reactions has become an emerging research theme due to their great potential in developing highly efficient catalysts or catalysts with high selectivity to substrates. For example, the conjugated structure of PDA has a synergistic effect with most semiconductor catalysts. The tunable surface charge can lead to a pronounced charge-dependent catalytic activity.[105,106] Besides, the combination of the unique properties of the photo-thermal responsive PDA with catalytically active metal NPs becomes an attractive goal to achieve responsive nanoreactors. Very recently, the unique photothermal conversion properties have been demonstrated to promote an advanced, controllable catalytic reaction for the reduction of 4-nitrophenol (Fig. 6a–c).[34] A catalytically active PDA@Au nanoreactor with a multi-compartment structure using porous PS-*b*-P2VP nanospheres as a soft template was synthesized. When applied for the reduction of 4-nitrophenol by $NaBH_4$, a remarkable acceleration of the reaction upon near-infrared irradiation was demonstrated. The authors speculated that the local surface temperature of the Au NPs under NIR irradiation was higher than that of the water bath environment. The preservation of the local heat on the surface of Au NPs by the PDA layers may be crucial to continuously generate a higher temperature in the nanoreactor than in the bulk solution. Given that the PDA complex structure plays a pivotal part in enhancing the catalytic activity under NIR irradiation, determining the relationship between the structural features and the photothermal properties, such as the photothermal conversion efficiency and the heat preservation effect,

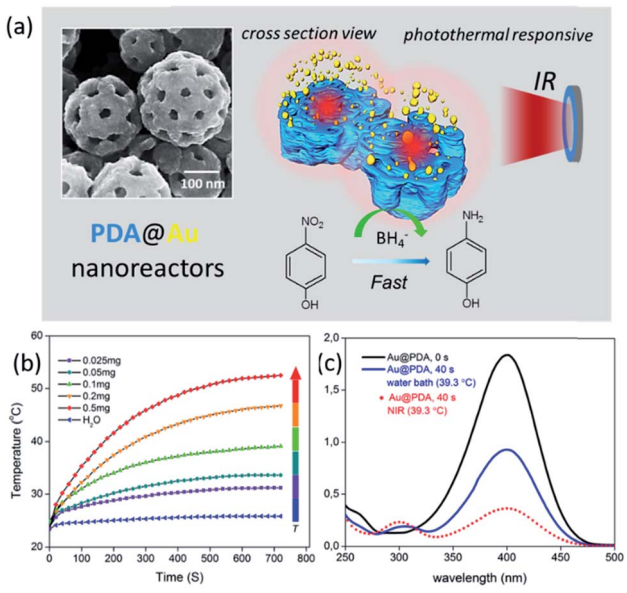

Fig. 6 (a) Morphology of the PDA@Au particles and their application as catalytic nanoreactors for the reduction of 4-nitrophenol under NIR irradiation. (b) Photothermal conversion properties of the nanoreactors. (c) Remarkable acceleration of the reduction of 4-nitrophenol under NIR irradiation. Reproduced with permission,[34] CCBY.

has become of great importance, and calls for systematic experimental and theoretical studies.

4.2.2 PDA as a direct catalyst. The presence of both acidic (phenolic OH) and basic (primary and secondary amines) functional groups enables the catalytic versatility of PDA, which can act in a cooperative fashion in the activation of reagents. The synergistic activation of both the electrophile and the nucleophile is considered to be a key factor in the PDA catalyzed aldol reaction between aromatic aldehydes and cyclohexanone.[107] Similar to the aldol reaction, the proximity of the acidic and basic functional groups of PDA is beneficial in the transformation of epoxides and CO_2 into cyclic carbonates.[108] Reaction under aqueous conditions has also been demonstrated, such as the synthesis of disulfides by aqueous thiol coupling.[109] Recently, the catalytic activity of PDA as an amine oxidase mimic has been reported for the synthesis of benzimidazoles, quinoxalines, and quinazolinones and oxidation of secondary amines.[110] Different from the supporting material for a metallic catalyst, PDA cannot be considered as an inert component or coating as it can generate reactivity. Generally, PDA itself as a catalyst has been less explored compared to PDA supported metallic catalysts especially in the form of nanoreactors. As a matter of fact, spatial confinement at the nanoscale created by PDA-based nanoreactors might have an additional effect on the kinetics and mechanisms of certain reactions, which can be a new topic of interest that has not been fully studied up to now.

4.3 Solar energy harvesting and utilization

The efficient harvesting and conversion of sunlight is crucial to maximize the utilization of solar energy. In general, solar energy can be harnessed and converted into various kinds of energy, including electricity, fuels and thermal energy, through photovoltaic, photochemical and photothermal processes, respectively.[111] Dye-sensitized solar cells (DSSCs) hold great promise in future photovoltaic applications due to their high energy conversion efficiencies and low production cost.[112] DSSCs are based on the light adsorption behavior of photosensitizing dyes coated atop a wide bandgap semiconductor (such as TiO_2). Taking advantage of the wide band absorption nature of PDA, nanoreactors creating good contact of PDA with the conducting metal oxide surface enable strong enhancement of solar energy harvesting. For example, PDA@TiO_2 core–shell nanostructures were reported to exhibit efficient dye-to-TiO_2 charge transfer.[113] Different from conventional DSSCs in which the electron injection typically takes place from the LUMO level of the dye to the conduction band (CB) of TiO_2 through a two-step process under photoexcitation, the efficient electron injection for PDA-based DSSCs followed a one-step direct charge transfer process. In other words, the photon injected through the transparent conducting oxide layer was transferred from the HOMO energy level of PDA to the CB of TiO_2 NPs upon photoexcitation.

Photothermal conversion is a direct conversion process of solar irradiation into heat that has attained the highest achievable conversion efficiency among the abovementioned energy conversion types. Therefore, solar steam generation, which desalinates/distills water using sunlight-powered evaporation with minimum environmental impact, has been widely investigated.[111,114] The combination of a well-designed nanostructure and the intrinsic photothermal conversion capability of the employed materials is a practical route to develop their performance in solar steam generation. Therefore, PDA-based photothermal conversion nanoreactors with the following advantages stand out as promising candidates: broadband and efficient light absorption (99% of incident photon energy over a broad solar spectrum (210–800 nm)),[114] heat localization or thermal insulation (low thermal conductivity to suppress thermal conduction away from the hot internal region), hydrophilicity, and interconnected pores. However, in the near infrared region (>800 nm), PDA itself has solar irradiation absorption of ~60%, which may not be sufficient for the utilization of light in the entire solar irradiation spectrum. Therefore, regarding solar-driven interfacial evaporation applications, it is necessary to increase the irradiation absorption capability of PDA in a wide wavelength range by introducing additional photothermal conversion agents. A recent study has demonstrated a broadened, large photothermal light absorption (~96%) *via* application of well-defined core–shell PDA@MXene microspheres and a piece of PVDF filter membrane as a wide spectrum light absorber for highly efficient solar driven interfacial evaporation.[115] The introduction of MXene significantly broadened the light absorption range of melanin-like PDA, while the unique wrapping structure provided ample water transportation channels *via* the gaps between the microspheres. The work not only provided a novel strategy to construct MXene/polymer multifunctional composite architectures, but also showed great promise in the field of solar-to-vapor generation for solving the water scarcity problem.

5. Perspectives

Although an impressively large number of studies have been carried out and the applications related to PDA nanoreactors are highly expected to reach the market, there are still obstacles blocking the transfer from fundamental study to practical applications due to a few key issues that must be primarily resolved. The challenges highlighted below may serve as guidance to future research over the next decades.

The first not-fully addressed issue under study is the polymerization mechanisms for different synthetic routes. Despite decades of increasing investigations, there is still a lack of final verdict with regard to the polymerization process, the precise structure, and the components of PDA. Moreover, the structure of PDA varies largely with reaction conditions, and significantly affects the properties and functions of PDA.

The second is that alternative synthetic strategies beyond the conventional solution oxidation method are in urgent need of development to increase the library of PDA products. For instance, as an environmentally benign procedure, the enzyme-catalyzed method based on an enzymatic oxidation process has aroused growing interest. The synthesized PDA usually entraps the oxidase residual with preserved enzymatic activity, making

it appealing for bio-applications. Apart from biological routes, a direct copolymerization strategy has been developed very recently to tune the light absorption properties *via* formation of 2,2,6,6-tetramethylpiperidine-1-oxyl (TEMPO)-doped 5,6-dihydroxyindole (DHI)/indole-5,6-quinone (IQ) oligomers.[116] These novel synthetic strategies imply that rational design of both monomer and polymer structures could pave the way to tune the intrinsic properties of PDA.

The third is how to break through the long-standing bottleneck in the synthesis of advanced nanoreactors with well-designed complex structures. Although their versatile adhesion to diverse substrates facilitates the use of hard templates for complex nanostructures, the harsh conditions required for the removal of most hard templates hinder the real application of various templates. Therefore, continual efforts dedicated to exploring more simple and effective methods for complex nanoreactors are highly desired.

Biomedical applications of PDA also require a detailed understanding of its interactions with biological systems. How it reacts with living cells, hormones, proteins, or immune systems is fundamental to the long-term clinical and commercial viability. Another important point is how PDA is biodegraded and eliminated from the body, specifically whether its byproducts are subject to accumulation within cells or organs.

In addition, PDA-based catalytic nanoreactors have not been fully exploited in organic synthesis. There are different functional groups in the polymer structure which could be further modified to build in additional functional groups or hybrid complexes. Most importantly, PDA could also be applied in photothermal conversion systems where the kinetics triggered by the photothermally converted heat could exhibit unexpected effects beyond current state-of-the-art applications. However, this potential has been less exploited so far. The underlying challenges may exist in at least, but not limited to, the determination of the structure–property relationship of PDA nanoreactors with regard to photothermal conversion efficiency and temperature preserving effect. Other challenges would be the determination of local temperature at the catalyst surface at the nanoscale, as well as that of the resulting heterogeneous thermal environment. Further development of smart nanoreactors with tunable catalytic activities that directly respond to light stimuli would be of special interest and a new trend for future nanoreactors based on a combination of PDA with photothermal conversion properties and thermal-responsive polymers.

In the case of electrochemical energy storage, the extended application of PDA in multifunctional composite materials creates many opportunities in advanced energy fields. For example, conducting polymers such as polyaniline and polypyrrole are widely used in lithium batteries. When incorporated with PDA, the composite polymers possess synergistic effects including adhesion, enhanced conductivity and charge storage capacity. Additionally, PDA is a versatile platform that can integrate with various MOFs, doping agents, and polyoxometalates, all of which can easily yield high-performance metallic or multi-metallic compounds for electrocatalysis and energy storage.

In conclusion, we anticipate that this review will not only provide readers with a panoramic view of PDA-based materials and systems for biomedicine, energy and catalysis applications, but also inspire researchers to develop more strategies for the design and synthesis of PDA nanoreactors with diverse properties and functions, further expanding their application scope in bioscience, energy, and other fields.

Conflicts of interest

There are no conflicts to declare.

Acknowledgements

Y.L. thanks the Deutsche Forschungsgemeinschaft (DFG, German Research Foundation – Project number 410871749) for financial support. X.X. acknowledges the Princeton Presidential Postdoctoral Fellowship Program for support. R.D.P. acknowledges the support of an NSF PFI Grant (IIP – 1827506).

Notes and references

1 H. Lee, S. M. Dellatore, W. M. Miller and P. B. Messersmith, *Science*, 2007, **318**, 426–430.
2 Y. L. Liu, K. L. Ai and L. H. Lu, *Chem. Rev.*, 2014, **114**, 5057–5115.
3 V. Ball, *Front Bioeng. Biotechnol.*, 2018, **6**, 109.
4 K. G. Qu, Y. H. Wang, A. Vasileff, Y. Jiao, H. Y. Chen and Y. Zheng, *J. Mater. Chem. A*, 2018, **6**, 21827–21846.
5 H. Sun, Y. Hong, Y. Xi, Y. Zou, J. Gao and J. Du, *Biomacromolecules*, 2018, **19**, 1701.
6 M. d'Ischia, A. Napolitano, A. Pezzella, P. Meredith and T. Sarna, *Angew. Chem., Int. Ed.*, 2009, **48**, 3914–3921.
7 M. d'Ischia, A. Napolitano, V. Ball, C. T. Chen and M. J. Buehler, *Acc. Chem. Res.*, 2014, **47**, 3541–3550.
8 J. Liebscher, R. Mrowczynski, H. A. Scheidt, C. Filip, N. D. Hadade, R. Turcu, A. Bende and S. Beck, *Langmuir*, 2013, **29**, 10539–10548.
9 J. H. Ryu, P. B. Messersmith and H. Lee, *ACS Appl. Mater. Interfaces*, 2018, **10**, 7523–7540.
10 H. A. Lee, Y. F. Ma, F. Zhou, S. Hong and H. Lee, *Acc. Chem. Res.*, 2019, **52**, 704–713.
11 Q. Wei, F. L. Zhang, J. Li, B. J. Li and C. S. Zhao, *Polym. Chem.*, 2010, **1**, 1430–1433.
12 F. Ponzio and V. Ball, *Colloids Surf., A*, 2014, **443**, 540–543.
13 W. Zheng, H. Fan, L. Wang and Z. Jin, *Langmuir*, 2015, **31**, 11671–11677.
14 J. L. Wang, B. C. Li, Z. J. Li, K. F. Ren, L. J. Jin, S. M. Zhang, H. Chang, Y. X. Sun and J. Ji, *Biomaterials*, 2014, **35**, 7679–7689.
15 D. Q. Fan, C. T. Wu, K. Wang, X. X. Gu, Y. Q. Liu and E. K. Wang, *Chem. Commun.*, 2016, **52**, 406–409.
16 K. L. Ai, Y. L. Liu, C. P. Ruan, L. H. Lu and G. Q. Lu, *Adv. Mater.*, 2013, **25**, 998–1003.
17 H. Sun, Y. Hong, Y. Xi, Y. Zou, J. Gao and J. Du, *Biomacromolecules*, 2018, **19**, 1701–1720.
18 X. Yu, H. L. Fan, L. Wang and Z. X. Jin, *Angew. Chem., Int. Ed.*, 2014, **53**, 12600–12604.

19 R. J. Li, K. Parvez, F. Hinkel, X. L. Feng and K. Mullen, *Angew. Chem., Int. Ed.*, 2013, **52**, 5535–5538.
20 H. Li, Y. Y. Zhao, Y. Jia, C. T. Qu and J. B. Li, *Chem. Commun.*, 2019, **55**, 15057–15060.
21 Y. Tokura, S. Harvey, C. J. Chen, Y. Z. Wu, D. Y. W. Ng and T. Weil, *Angew. Chem., Int. Ed.*, 2018, **57**, 1587–1591.
22 F. Chen, Y. X. Xing, Z. Q. Wang, X. Y. Zheng, J. X. Zhang and K. Y. Cai, *Langmuir*, 2016, **32**, 12119–12128.
23 H. Kim, D. W. Kim, V. Vasagar, H. Ha, S. Nazarenko and C. J. Ellison, *Adv. Funct. Mater.*, 2018, **28**, 1803172.
24 R. Liu, S. M. Mahurin, C. Li, R. R. Unocic, J. C. Idrobo, H. J. Gao, S. J. Pennycook and S. Dai, *Angew. Chem., Int. Ed.*, 2011, **50**, 6799–6802.
25 L. Zhang, C. Chang, C. W. Hsu, C. W. Chang and S. Y. Lu, *J. Mater. Chem. A*, 2017, **5**, 19656–19663.
26 K. G. Qu, Y. H. Wang, X. X. Zhang, H. Y. Chen, H. B. Li, B. L. Chen, H. W. Zhou, D. C. Li, Y. Zheng and S. Dai, *ChemNanoMat*, 2018, **4**, 417–422.
27 B. Y. Guan, S. L. Zhang and X. W. Lou, *Angew. Chem., Int. Ed.*, 2018, **57**, 6176–6180.
28 D. W. Wan, C. R. Yan and Q. Y. Zhang, *Ind. Eng. Chem. Res.*, 2019, **58**, 16358–16369.
29 J. Cao, S. L. Mei, H. Jia, A. Ott, M. Ballauff and Y. Lu, *Langmuir*, 2015, **31**, 9483–9491.
30 M. Arzillo, G. Mangiapia, A. Pezzella, R. K. Heenan, A. Radulescu, L. Paduano and M. d'Ischia, *Biomacromolecules*, 2012, **13**, 2379–2390.
31 M. Mateescu, M. H. Metz-Boutigue, P. Bertani and V. Ball, *J. Colloid Interface Sci.*, 2016, **469**, 184–190.
32 A. Chassepot and V. Ball, *J. Colloid Interface Sci.*, 2014, **414**, 97–102.
33 J. Cui, Y. Wang, A. Postma, J. Hao, L. Hosta-Rigau and F. Caruso, *Adv. Funct. Mater.*, 2010, **20**, 1625–1631.
34 S. L. Mei, Z. Kochovski, R. Roa, S. S. Gu, X. H. Xu, H. T. Yu, J. Dzubiella, M. Ballauff and Y. Lu, *Nano-Micro Lett.*, 2019, **11**, 83.
35 R. Solaro, F. Chiellini and A. Battisti, *Materials*, 2010, **3**, 1928–1980.
36 D. R. Dreyer, D. J. Miller, B. D. Freeman, D. R. Paul and C. W. Bielawski, *Langmuir*, 2012, **28**, 6428–6435.
37 F. Y. Liu, X. X. He, Z. Lei, L. Liu, J. P. Zhang, H. P. You, H. M. Zhang and Z. X. Wang, *Adv. Healthcare Mater.*, 2015, **4**, 559–568.
38 N. Wang, Y. Yang, X. L. Wang, X. X. Tian, W. J. Qin, X. X. Wang, J. Y. Liang, H. L. Zhang and X. G. Leng, *ACS Biomater. Sci. Eng.*, 2019, **5**, 2330–2342.
39 C. C. Ho and S. J. Ding, *J. Mater. Sci.: Mater. Med.*, 2013, **24**, 2381–2390.
40 X. Y. Wang, J. S. Zhang, Y. T. Wang, C. P. Wang, J. R. Xiao, Q. Zhang and Y. Y. Cheng, *Biomaterials*, 2016, **81**, 114–124.
41 R. Liu, Y. L. Guo, G. Odusote, F. L. Qu and R. D. Priestley, *ACS Appl. Mater. Interfaces*, 2013, **5**, 9167–9171.
42 C. A. H. Thompson, A. Gu, S. Y. Yang, V. Mathew, H. B. Fleisig and J. M. Y. Wong, *Mol. Cancer Res.*, 2018, **16**, 1215–1225.
43 L. Dong, C. Wang, W. Y. Zhen, X. D. Jia, S. J. An, Z. A. Xu, W. Zhang and X. E. Jiang, *J. Mater. Chem. B*, 2019, **7**, 6172–6180.
44 D. Wu, J. J. Zhou, X. H. Chen, Y. H. Chen, S. Hou, H. H. Qian, L. F. Zhang, G. P. Tang, Z. Chen, Y. Ping, W. J. Fang and H. W. Duan, *Biomaterials*, 2020, **238**, 119847.
45 P. A. Rühs, K. G. Malollari, M. R. Binelli, R. Crockett, D. W. R. Balkenende, A. R. Studart and P. B. Messersmith, *ACS Nano*, 2020, **14**, 3885–3895.
46 J. Park, T. F. Brust, H. J. Lee, S. C. Lee, V. J. Watts and Y. Yeo, *ACS Nano*, 2014, **8**, 3347–3356.
47 Y. H. Fan, Y. Zhang, Q. Zhao, Y. H. Xie, R. F. Luo, P. Yang and Y. J. Weng, *Biomaterials*, 2019, **204**, 36–45.
48 B. Yu, D. A. Wang, Q. Ye, F. Zhou and W. M. Liu, *Chem. Commun.*, 2009, 6789–6791.
49 J. W. Cui, Y. Yan, G. K. Such, K. Liang, C. J. Ochs, A. Postma and F. Caruso, *Biomacromolecules*, 2012, **13**, 2225–2228.
50 F. Y. Li, H. Yang, N. N. Bie, Q. B. Xu, T. Y. Yong, Q. Wang, L. Gan and X. L. Yang, *ACS Appl. Mater. Interfaces*, 2017, **9**, 23564–23573.
51 M. Qiu, D. Wang, W. Y. Liang, L. P. Liu, Y. Zhang, X. Chen, D. K. Sang, C. Y. Xing, Z. J. Li, B. Q. Dong, F. Xing, D. Y. Fan, S. Y. Bao, H. Zhang and Y. H. Cao, *Proc. Natl. Acad. Sci. U. S. A.*, 2018, **115**, 501–506.
52 H. Y. Mao, S. Laurent, W. Chen, O. Akhavan, M. Imani, A. A. Ashkarran and M. Mahmoudi, *Chem. Rev.*, 2013, **113**, 3407–3424.
53 Y. L. Liu, K. L. Ai, J. H. Liu, M. Deng, Y. Y. He and L. H. Lu, *Adv. Mater.*, 2013, **25**, 1353–1359.
54 D. H. Hu, C. B. Liu, L. Song, H. D. Cui, G. H. Gao, P. Liu, Z. H. Sheng and L. T. Cai, *Nanoscale*, 2016, **8**, 17150–17158.
55 N. Li, T. T. Li, C. Hu, X. M. Lei, Y. P. Zuo and H. Y. Han, *ACS Appl. Mater. Interfaces*, 2016, **8**, 15013–15023.
56 Z. L. Dong, H. Gong, M. Gao, W. W. Zhu, X. Q. Sun, L. Z. Feng, T. T. Fu, Y. G. Li and Z. Liu, *Theranostics*, 2016, **6**, 1031–1042.
57 R. Zheng, S. Wang, Y. Tian, X. G. Jiang, D. L. Fu, S. Shen and W. L. Yang, *ACS Appl. Mater. Interfaces*, 2015, **7**, 15876–15884.
58 F. Ding, X. H. Gao, X. G. Huang, H. Ge, M. Xie, J. W. Qian, J. Song, Y. H. Li, X. Y. Zhu and C. Zhang, *Biomaterials*, 2020, **245**, 119976.
59 Y. P. Li, W. Y. Hong, H. N. Zhang, T. T. Zhang, Z. Y. Chen, S. L. Yuan, P. Peng, M. Xiao and L. Xu, *J. Controlled Release*, 2020, **317**, 232–245.
60 R. Chen, C. Zhu, Y. Fan, W. Feng, J. Wang, E. Shang, Q. Zhou and Z. Chen, *ACS Appl. Bio Mater.*, 2019, **2**, 874–883.
61 W. Ding, L. Li, K. Xiong, Y. Wang, W. Li, Y. Nie, S. G. Chen, X. Q. Qi and Z. D. Wei, *J. Am. Chem. Soc.*, 2015, **137**, 5414–5420.
62 Y. Z. Sun and E. W. Davis, *J. Mater. Chem. B*, 2019, **7**, 6828–6839.
63 Y. X. Xing, J. X. Zhang, F. Chen, J. J. Liu and K. Y. Cai, *Nanoscale*, 2017, **9**, 8781–8790.
64 D. Wu, X. H. Duan, Q. Q. Guan, J. Liu, X. Yang, F. Zhang, P. Huang, J. Shen, X. T. Shuai and Z. Cao, *Adv. Funct. Mater.*, 2019, **29**, 1900095.
65 G. Yeroslavsky, M. Richman, L.-o. Dawidowicz and S. Rahimipour, *Chem. Commun.*, 2013, **49**, 5721–5723.

66 G. Yeroslavsky, R. Lavi, A. Alishaev and S. Rahimipour, *Langmuir*, 2016, **32**, 5201–5212.
67 Y. Cong, T. Xia, M. Zou, Z. N. Li, B. Peng, D. Z. Guo and Z. W. Deng, *J. Mater. Chem. B*, 2014, **2**, 3450–3461.
68 Z. S. Lu, J. Xiao, Y. Wang and M. Meng, *J. Colloid Interface Sci.*, 2015, **452**, 8–14.
69 Z. Zhang, J. Zhang, B. Zhang and J. Tang, *Nanoscale*, 2013, **5**, 118–123.
70 T. S. Sileika, H.-D. Kim, P. Maniak and P. B. Messersmith, *ACS Appl. Mater. Interfaces*, 2011, **3**, 4602–4610.
71 Y. Ren, J. G. Rivera, L. He, H. Kulkarni, D.-K. Lee and P. B. Messersmith, *BMC Biotechnol.*, 2011, **11**, 63.
72 G. Yeroslavsky, O. Girshevitz, J. Foster-Frey, D. M. Donovan and S. Rahimipour, *Langmuir*, 2015, **31**, 1064–1073.
73 K. Patel, P. Kushwaha, S. Kumar and R. Kumar, *ACS Appl. Bio Mater.*, 2019, **2**, 5799–5809.
74 D. Park, J. Kim, Y. M. Lee, J. Park and W. J. Kim, *Adv. Healthcare Mater.*, 2016, **5**, 2019–2024.
75 N. N. M. Adnan, Z. Sadrearhami, A. Bagheri, T. K. Nguyen, E. H. H. Wong, K. K. K. Ho, M. Lim, N. Kumar and C. Boyer, *Macromol. Rapid Commun.*, 2018, **39**, 1800159.
76 Z. Sadrearhami, F. N. Shafiee, K. K. K. Ho, N. Kumar, M. Krasowska, A. Blencowe, E. H. H. Wong and C. Boyer, *ACS Appl. Mater. Interfaces*, 2019, **11**, 7320–7329.
77 W. X. Lei, K. F. Ren, T. T. Chen, X. C. Chen, B. C. Li, H. Chang and J. Ji, *Adv. Mater. Interfaces*, 2016, **3**, 1600767.
78 J. L. Song, H. Liu, M. Lei, H. Q. Tan, Z. Y. Chen, A. Antoshin, G. F. Payne, X. Qu and C. S. Liu, *ACS Appl. Mater. Interfaces*, 2020, **12**, 8915–8928.
79 K. Ma, P. Dong, M. J. Liang, S. S. Yu, Y. Y. Chen and F. Wang, *ACS Appl. Mater. Interfaces*, 2020, **12**, 6955–6965.
80 S. M. Yu, G. W. Li, R. Liu, D. Ma and W. Xue, *Adv. Funct. Mater.*, 2018, **28**, 1707440.
81 S. W. Lee, N. Yabuuchi, B. M. Gallant, S. Chen, B. S. Kim, P. T. Hammond and Y. Shao-Horn, *Nat. Nanotechnol.*, 2010, **5**, 531–537.
82 M. H. Ryou, Y. M. Lee, J. K. Park and J. W. Choi, *Adv. Mater.*, 2011, **23**, 3066.
83 M. H. Ryou, D. J. Lee, J. N. Lee, Y. M. Lee, J. K. Park and J. W. Choi, *Adv. Energy Mater.*, 2012, **2**, 645–650.
84 Y. He, H. W. Xu, J. L. Shi, P. Y. Liu, Z. Q. Tian, N. Dong, K. Luo, X. F. Zhou and Z. P. Liu, *Energy Storage Mater.*, 2019, **23**, 418–426.
85 Q. Q. Meng, H. M. Zhang, Y. Liu, S. B. Huang, T. Z. Zhou, X. F. Yang, B. Y. Wang, W. F. Zhang, H. Ming, Y. Xiang, M. Li, G. P. Cao, Y. Q. Huang, L. Z. Fang, H. Zhang and Y. P. Guan, *Nano Res.*, 2019, **12**, 2919–2924.
86 L. Wang, D. Wang, Z. Dong, F. Zhang and J. Jin, *Nano Lett.*, 2013, **13**, 1711–1716.
87 Z. C. Liu, J. L. Huang, X. W. Zhao, H. Y. Huang, C. C. Fu, Z. H. Li, Y. H. Cheng, C. M. Niu and J. Y. Zhang, *ChemPlusChem*, 2019, **84**, 203–209.
88 D. Gueon and J. H. Moon, *Chem. Commun.*, 2019, **55**, 361–364.
89 T. Li, X. Bai, U. Gulzar, Y. J. Bai, C. Capiglia, W. Deng, X. F. Zhou, Z. P. Liu, Z. F. Feng and R. P. Zaccaria, *Adv. Funct. Mater.*, 2019, **29**, 1901730.
90 W. Zhou, X. Xiao, M. Cai and L. Yang, *Nano Lett.*, 2014, **14**, 5250–5256.
91 Z. J. Fan, B. Ding, H. S. Guo, M. Y. Shi, Y. D. Zhang, S. Y. Dong, T. F. Zhang, H. Dou and X. G. Zhang, *Chem. –Eur. J.*, 2019, **25**, 10710–10717.
92 X. Q. Zhang, D. Xie, Y. Zhong, D. H. Wang, J. B. Wu, X. L. Wang, X. H. Xia, C. D. Gu and J. P. Tu, *Chem. –Eur. J.*, 2017, **23**, 10610–10615.
93 Y. F. Deng, H. Xu, Z. W. Bai, B. L. Huang, J. Y. Su and G. H. Chen, *J. Power Sources*, 2015, **300**, 386–394.
94 T. Tang, W.-J. Jiang, X.-Z. Liu, J. Deng, S. Niu, B. Wang, S.-F. Jin, Q. Zhang, L. Gu, J.-S. Hu and L.-J. Wan, *J. Am. Chem. Soc.*, 2020, **142**, 7116–7127.
95 T. Sun, Z. J. Li, H. G. Wang, D. Bao, F. L. Meng and X. B. Zhang, *Angew. Chem., Int. Ed.*, 2016, **55**, 10662–10666.
96 J. H. Huang, Z. H. Yang, R. J. Wang, Z. Zhang, Z. B. Feng and X. E. Xie, *J. Mater. Chem. A*, 2015, **3**, 7429–7436.
97 J. Shin, J. Lee, Y. Park and J. W. Choi, *Chem. Sci.*, 2020, **11**, 2028–2044.
98 Q. Zhao, W. W. Huang, Z. Q. Luo, L. J. Liu, Y. Lu, Y. X. Li, L. Li, J. Y. Hu, H. Ma and J. Chen, *Sci. Adv.*, 2018, **4**, eaao1761.
99 X. Yue, H. Liu and P. Liu, *Chem. Commun.*, 2019, **55**, 1647–1650.
100 A. Molnar, *ChemCatChem*, 2020, **12**, 2649–2689.
101 A. Kunfi and G. London, *Synthesis*, 2019, **51**, 2829–2838.
102 J. J. Zhou, B. Duan, Z. Fang, J. B. Song, C. X. Wang, P. B. Messersmith and H. W. Duan, *Adv. Mater.*, 2014, **26**, 701–705.
103 A. V. Dubey and A. V. Kumar, *RSC Adv.*, 2016, **6**, 46864–46870.
104 A. Kunfi, Z. May, P. Nemeth and G. London, *J. Catal.*, 2018, **361**, 84–93.
105 A. J. Ma, Y. J. Xie, J. Xu, H. B. Zeng and H. L. Xu, *Chem. Commun.*, 2015, **51**, 1469–1471.
106 X. Han, X. L. Chen, M. F. Yan and H. L. Liu, *Particuology*, 2019, **44**, 63–70.
107 R. Mrowczynski, A. Bunge and J. Liebscher, *Chem. –Eur. J.*, 2014, **20**, 8647–8653.
108 Z. F. Yang, J. Sun, X. M. Liu, Q. Su, Y. Liu, Q. Li and S. J. Zhang, *Tetrahedron Lett.*, 2014, **55**, 3239–3243.
109 Y. Du, H. C. Yang, X. L. Xu, J. Wu and Z. K. Xu, *ChemCatChem*, 2015, **7**, 3822–3825.
110 S. A. Pawar, A. N. Chand and A. V. Kumar, *ACS Sustainable Chem. Eng.*, 2019, **7**, 8274–8286.
111 L. L. Zhu, M. M. Gao, C. K. N. Peh and G. W. Ho, *Mater. Horiz.*, 2018, **5**, 323–343.
112 M. Gratzel, *Nature*, 2001, **414**, 338–344.
113 H. J. Nam, B. Kim, M. J. Ko, M. Jin, J. M. Kim and D. Y. Jung, *Chem. –Eur. J.*, 2012, **18**, 14000–14007.
114 Z. Wang, H.-C. Yang, F. He, S. Peng, Y. Li, L. Shao and S. B. Darling, *Matter*, 2019, **1**, 115–155.
115 X. Zhao, X.-J. Zha, L.-S. Tang, J.-H. Pu, K. Ke, R.-Y. Bao, Z.-y. Liu, M.-B. Yang and W. Yang, *Nano Res.*, 2020, **13**, 255–264.
116 Y. Zou, X. Chen, P. Yang, G. Liang, Y. Yang, Z. Gu and Y. Li, *Sci. Adv.*, 2020, **6**, eabb4696.